Supplemental Information

New structural motif and revised molecular basis of the promiscuous carboxylic acid perhydrolase activity in serine hydrolases

DeLu (Tyler) Yin, Vince Purpero, Ryota Fujii, Romas Kazlauskas

University of Minnesota, Department of Biochemistry, Molecular Biology & Biophysics and The Biotechnology Institute, 1479 Gortner Avenue, Saint Paul MN 55108 USA

Contents

Supplemental Data

Saturation mutagenesis at position 29. Saturation mutagenesis the 29 position of PFE creates the nineteen possible amino acid substitutions. Previous research characterized variant L29P [1-3] while variant L29R PFE could not be isolated. Nickel affinity chromatography purified the remaining seventeen L29X variants and they were assayed for hydrolysis of *p*-nitrophenyl acetate and perhydrolysis of acetic acid and ethyl acetate, Figure S1a. All seventeen remaining L29X variants catalyzed hydrolysis of *p*-nitrophenyl acetate, but the specific activity was lower than that of wild type, Figure S1b (dark grey bars). The variants with the highest activity were L29F (6.9 U/mg) and L29I (5.1 U/mg), which showed almost half the activity of the wild type (14 U/mg). Variants L29P (0.10 U/mg) and L29D (0.098 U/mg) showed the lowest activity, more than 100-fold lower than wild-type PFE. We previously suggested that steric hindrance accounts for the drop in hydrolysis activity for L29P[2].

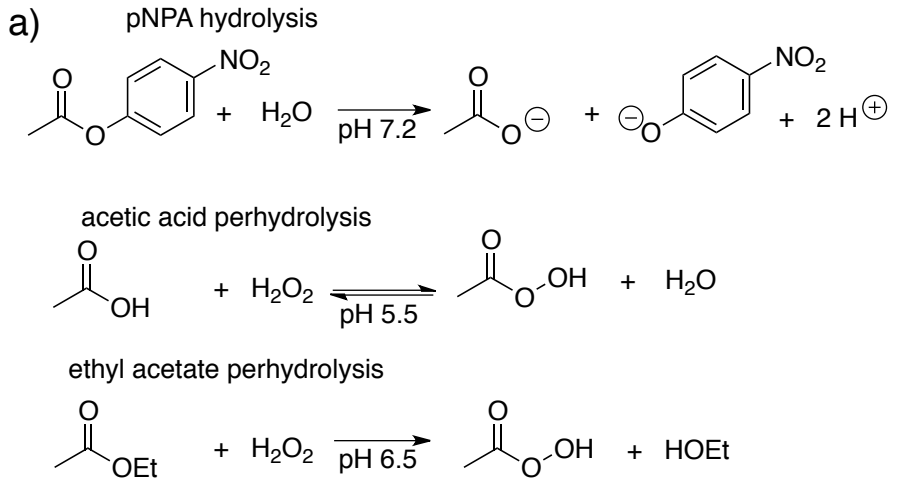

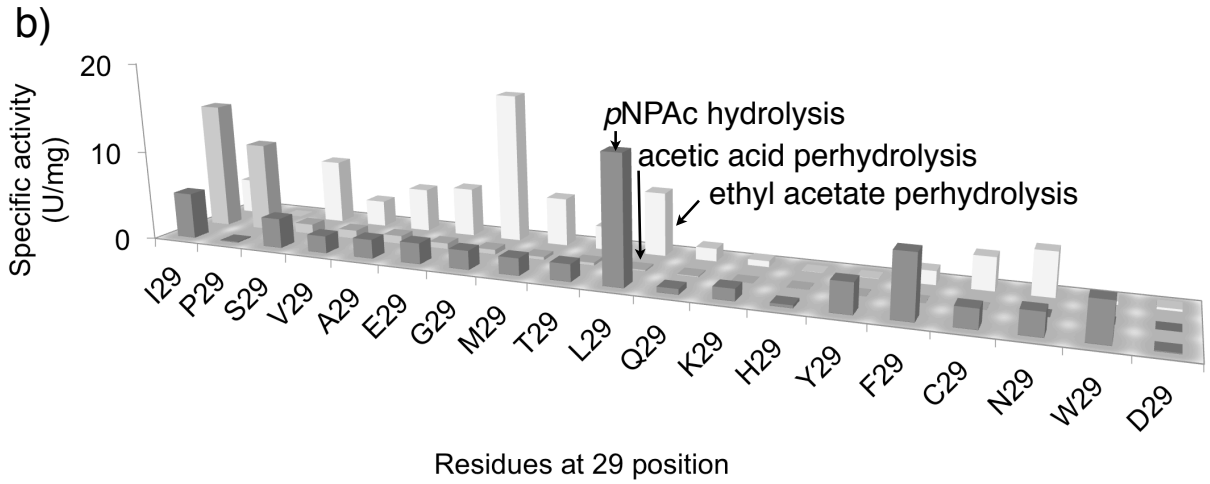

Figure S1. L29X catalyzed hydrolysis and perhydrolysis. a) Reaction scheme for L29X catalyzed hydrolysis and perhydrolysis. b) Initial rate of hydrolysis of *p*-nitrophenyl acetate (pNPAc; dark grey bars) and perhydrolysis of acetic acid (light grey bars) and ethyl acetate (white bars) catalyzed by L29X variants of *Pseudomonas fluorescens* esterase. Six variants catalyzed perhydrolysis of acetic acid at least four times faster than wild type: L29I (14 U/mg), L29P (9.9 U/mg), L29S (1.1 U/mg), L29V (0.96 U/mg), L29A (0.91 U/mg) and L29E (0.65 U/mg). Wild-type PFE is the best catalyst for hydrolysis (14 U/mg); L29I PFE (14 U/mg) is the best catalyst for perhydrolysis of acetic acid and L29G PFE is the best catalyst for perhydrolysis of ethyl acetate (17 U/mg).

Six of the eighteen L29X variants catalyzed perhydrolysis of acetic acid at least four times faster than wild type: L29I PFE (14 U/mg), L29P PFE (9.9 U/mg), L29S PFE (1.1 U/mg), L29V PFE (0.96 U/mg), L29A PFE (0.91 U/mg) and L29E PFE (0.65 U/mg), Figure 2b (light grey bars). This value for L29I PFE is 83-fold higher than wild type PFE (0.15 U/mg). This result is surprising because all carboxylic acid perhydrolases known until now contain a proline at position 29, not an isoleucine. Additionally, the apparently minor change of leucine to isoleucine caused such a large change in perhydrolysis activity. Three other variants showed a twofold increase in perhydrolysis activity (L29G, M, T), while the eleven remaining variants showed lower perhydroly-

sis activity than wild type. These changes in perhydrolysis of carboxylic acids over a >2000-fold range by amino acid substitutions at this position identifies this location as a key position for perhydrolysis.

For perhydrolysis of an ester, ethyl acetate, only one of the seventeen L29X variants was faster than wild type: L29G PFE (17 U/mg vs. 7.1 U/mg for wild-type PFE), Figure S1b (white bars). L29S PFE was equally active to wild-type, while L29I PFE was half as active as wild-type PFE. This is an unusual feature of L29I PFE: it is a good perhydrolase for both carboxylic acid and carboxylic acid esters. In other cases, esterases like PFE are good catalysts for perhydrolysis of esters, but not carboxylic acids, while perhydrolases like L29P PFE are good catalysts for perhydrolysis of carboxylic acids, but not esters. L29I PFE is good at both.

To measure the relative abilities of the twelve most active variants to catalyze perhydrolysis and hydrolysis, we used an ester substrate, ethyl acetate. Unlike carboxylic acids, an ester may undergo either perhydrolysis or hydrolysis and the relative amount of each product indicates the abilities of the enzyme. The ratio of perhydrolysis to hydrolysis of ethyl acetate for the L29X variants did not vary widely; all were within a factor of 5.5, Table S1. The highest ratio was a 2.1-fold preference for perhydrolysis by wild type PFE and the lowest was a 0.38-fold preference for perhydrolysis by L29P. The ratio for wild-type and L29P PFE is similar to the k_{cat}/K_m for perhydrolysis and hydrolysis of ethyl acetate measured by steady state kinetics. The ratio in Table 3 is relative amount of peracetic and acetic acids formed in the first 20 min of reaction; usually less than 10 mol% of the ethyl acetate had reacted, so this value is an initial ratio. In one case, L29I PFE, almost half of the ethyl acetate was consumed, so the assumption of initial rates does not hold. The measured ratio of 0.044 suggests that hydrolysis of peracetic acid is highly favored, but a more accurate measure of this ratio using steady state kinetic (see below) indicate that the correct value is 0.8.

Table S1. Relative amounts of peracetic and acetic acids formed during perhydrolysis of ethyl acetate catalyzed by PFE variants.[a]

PFE Variant	Peracetic Acid Formed, mM	Acetic Acid Formed, mM	Peracetic Acid/ Acetic Acid
WT	18	8.6	2.1 (2.7) [c]
L29A	20	33	0.61
L29C	17	27	0.64

L29F	19	17	1.1
L29G	24	29	0.86
L29I	11	260	0.044 (0.8) [c]
L29M	22	22	1.0
L29N	20	9.6	2.1
L29T	25	44	0.58
L29P[b]	14	54	0.38 (0.25) [c]
L29S	30	45	0.65
L29V	21	30	0.71

[a] Reaction conditions: enzyme, 0.1 mg/mL; 100 mM citrate buffer (pH 6.5); 250 mM H_2O_2; 600 mM ethyl acetate; 37 ºC; reaction time, 20 min; quenched with nine volumes of 50 mM H_3PO_4. [b] Methyl acetate was used as substrate because ethyl acetate is a very poor substrate for L29P PFE. [c] The values in parentheses are ratios of k_{cat}/K_m for perhydrolysis and hydrolysis of ethyl acetate measured by steady state kinetics. The two measurement methods should agree with each other. In the case of L29I PFE, they do not because the reaction continued to 50% conversion, well beyond the initial rate. L29I PFE-catalyzed hydrolysis of peracetic acid likely contributed to the high amount of acetic acid in this case.

Calibration curve for measuring acetic acid by HPLC. Solutions of known acetic acid concentration were analyzed by HPLC using an ACE 5 C18 column (250 × 4.6 mm) eluted with 0.1% H_3PO_4 and 20 mM H_2SO_4 at a flow rate of 0.5 mL/min. The acetic acid eluted at 10.5 min and the area of the peak detected by UV absorbance at 210 nm increased linearly with acetic acid concentration in the range 0.2 to 2.0 mM, Figure S1.

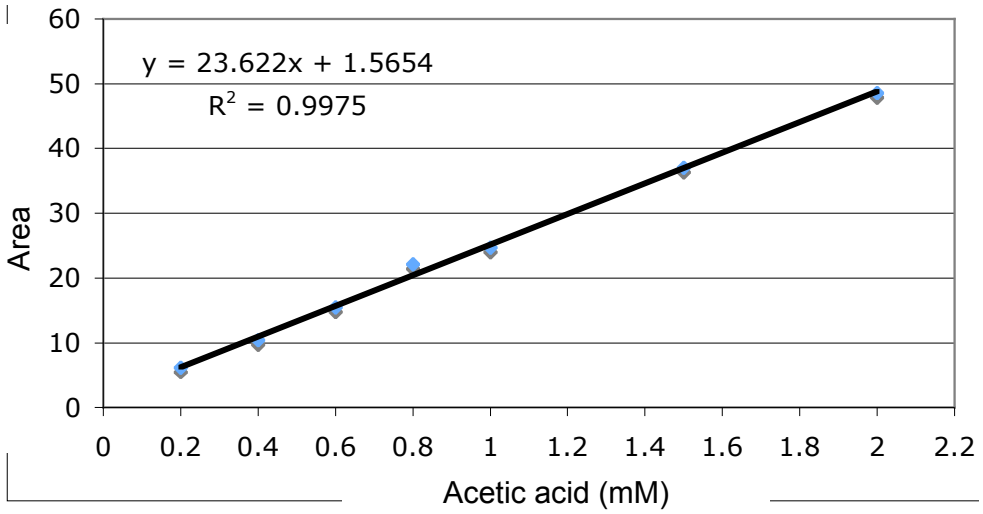

Figure S2. Calibration curve for measurement of acetic acid concentration by HPLC. The integrated peak areas measured by UV at 210 nm increased linearly with acetic acid concentration in the range of 0.2 to 2.0 mM. The line is a best fit with a slope of 23.6 and intercept of 1.5.

Steric interactions of L29I structures. Substitution of Leu with Ile at the 29 position of PFE creates internal steric clashes in both the type I or type II turn conformations, so neither conformation is favored. Similar clashes occur in the L29I PFE apo and L29I PFE/acetate structures. The crystal structures contain six nearly identical protein molecules labelled chain a-f. Representative structure are analyzed in Figure S3.

In the L29I PFE apo structure, the δ- and γ(1)-methyl groups lie close to each other. The C–C distance is 2.8 Å for the type I turn, Figure S2a, and 2.7 Å for the type II turn, Figure S3b. For comparison, the combined van der Waals radii of two methyl groups is 4.0 Å.[4] The γ(1)-methylene group of L29I clashes with the main-chain amide of I29 (2.7 Å), type I turn, Figure S3a, while it clashes with the main-chain carbonyl of W28 (2.8 Å) in the type II turn, Figure S3b. The β-methine clashes with the main chain carbonyl of I29. The C–O distance is 2.7 Å for both the type I turn, Figure S3a and the type II turn, Figure S3b, and the dihedral angle between these atoms is nearly eclipsed: 17.7˚ and 1.9˚.

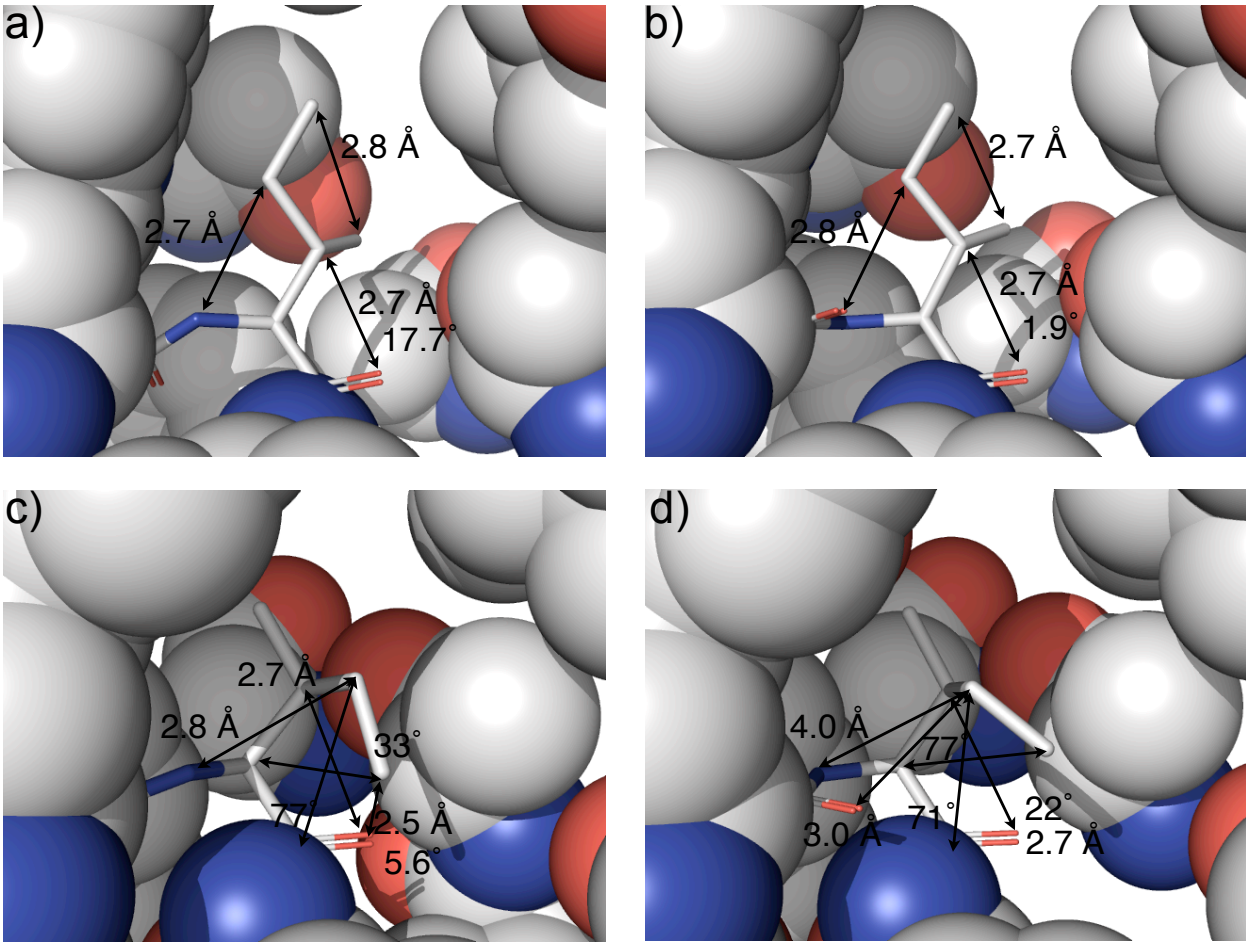

Figure S3. Similar steric clashes in the L29I PFE apo structures type I (a) and type II (b) conformations and in the L29I PFE/acetate structures type I (c) and type II (d). Residue Ile29 and the main chain carbonyl of Trp28 are shown in sticks. a) Chain c of L29I apo type I turn shows three steric clashes: 1) the side chain γ(1)-methylene of I29 and main chain amide of I29 (2.7 Å), 2) the side chain β-methine of I29 and carbonyl oxygen of I29 (2.7 Å), and 3) the side chain δ- and γ(1)-methyl groups of I29 (2.8 Å). b) Chain e of L29I apo type II turn shows three steric clashes: 1) the side chain γ(1)-methylene of I29 and main chain carbonyl oxygen of W28 (2.8 Å). 2) the side chain β-methine of I29 and carbonyl oxygen of I29 (2.7 Å) 3) the side chain δ- and γ(1)-methyl groups of I29 (2.7 Å). c) Chain c of L29I/acetate type I turn shows three steric clashes: 1) the γ(2)-methylene group and main chain amide of I29 (2.8 Å), 2) the β-methine group and the main chain carbonyl of I29 (2.7 Å), and 3) the δ-methyl group and the main chain carbonyl of I29 (2.5 Å). d) Chain d of L29I/acetate type II turn shows two steric clash: 1) the γ(2)-methylene group and main chain carbonyl oxygen of W28 (3.0 Å) and 2) the β-methine group and the main

chain carbonyl of I29 (2.7 Å). L29I/acetate for both type I, c) and II, d) turn show a *syn*-pentane interaction between the δ-methyl group and main chain carbonyl if I29.

The Ile29 side chain in the L29I PFE/acetate structure adopts a rotamer different from that in the L29I PFE apo structure, but it also contains several steric clashes.

In the L29I/acetate type I turn, γ(2)-methylene group and main chain amide of I29 lie close to each other; the C-N bond is 2.8 Å, Figure S3c. The β-methine clashes with the main chain carbonyl of I29; the C-O distance is 2.5 Å for the type I turn, Figure S3c.The δ-methyl group and the main chain carbonyl of I29 lie too close to each other, the C-C distance is 2.5 Å. A *syn*-pentane-type interaction is present between the δ-methyl group and main chain carbonyl of I29. The dihedral angles that form the *syn*-pentane interaction are: (C=O)-C(α)-C(β) = 5.6° and C(δ)-C(γ(2))-C(β)-C(α) = 33°.

In the type II turn of L29I/acetate, the β-methine clashes with the main chain carbonyl of I29. The C-O distance is 2.7 Å for the type II turn, Figure S3d. The γ(2)-methylene group clashes with the main chain carbonyl of W28, but not with the amide of W28. The C-O distance is 3.0 Å and the C-N distance is 4.0 Å. For comparison, the combined van der Waals radii of oxygen and methyl is 3.54 Å.[1] The β-methine group and the main chain carbonyl of I29 lie too close to each other; the C-O distance is 2.7 Å. A *syn*-pentane-type interaction is present between the δ-methyl group and main chain carbonyl of I29. The dihedral angles that form the *syn*-pentane interaction are: (C=O)-C(α)-C(β) = 22° and C(δ)-C(γ(2))-C(β)-C(α) = 77°.

Molecular modeling of L29I-T_d1 intermediate with either acetic acid or acetate. Modeling predicts ACT2 is in the acetate, not acetic acid form, to create a catalytic productive structure for L29I-T_d1. A catalytically productive T_dI structure must contain four key hydrogen bonds: the oxyanion of the tetrahedral intermediate accepts two hydrogen bonds from the main chain amides (M95 and W28) and the His-NεH donates two hydrogen bonds – one to hydroxyl group of the tetrahedral intermediate (T_d1-OH) and the same hydrogen to Ser-Oγ. This bifurcated hydrogen bond from His-NεH represents the removal of proton from Ser-Oγ-H and the donation of this proton to the T_d1s leaving OH.

The crystal structure of L29I/acetate contains two acetate molecules. We built models of T_d1 structures of L29I (type I and II turns) using the acetic acid (ACT1) while keeping the ace-

tate (ACT2) in the original orientation seen in the crystal structure. Next, we built additional models T_d1 with either type I or II turn by neutralizing ACT2 with a proton to form acetic acid, making a total of four structures with either type I or II turns and different ionization states for ACT2. We optimized the geometry of all four structures using the OPLS 2005 forcefield[5] in the Macromodel v 9.1 (Schrödinger, New York) program until an rmsd of <0.05 Å was reached.

The L29I-T_d1 intermediate with acetate forms these four hydrogen bonds as well as three others involving the ionized form of ACT2, Figure S4a. The acetate accepts three hydrogen bonds: one from the Td1-OH and two from main chain amides (I29 and L30). The hydrogen bond between Td1-OH and the carboxylate group of acetate promote water release, thus favoring the formation of the acetyl enzyme. This structure represents the molecular basis of how L29I increases perhydrolysis.

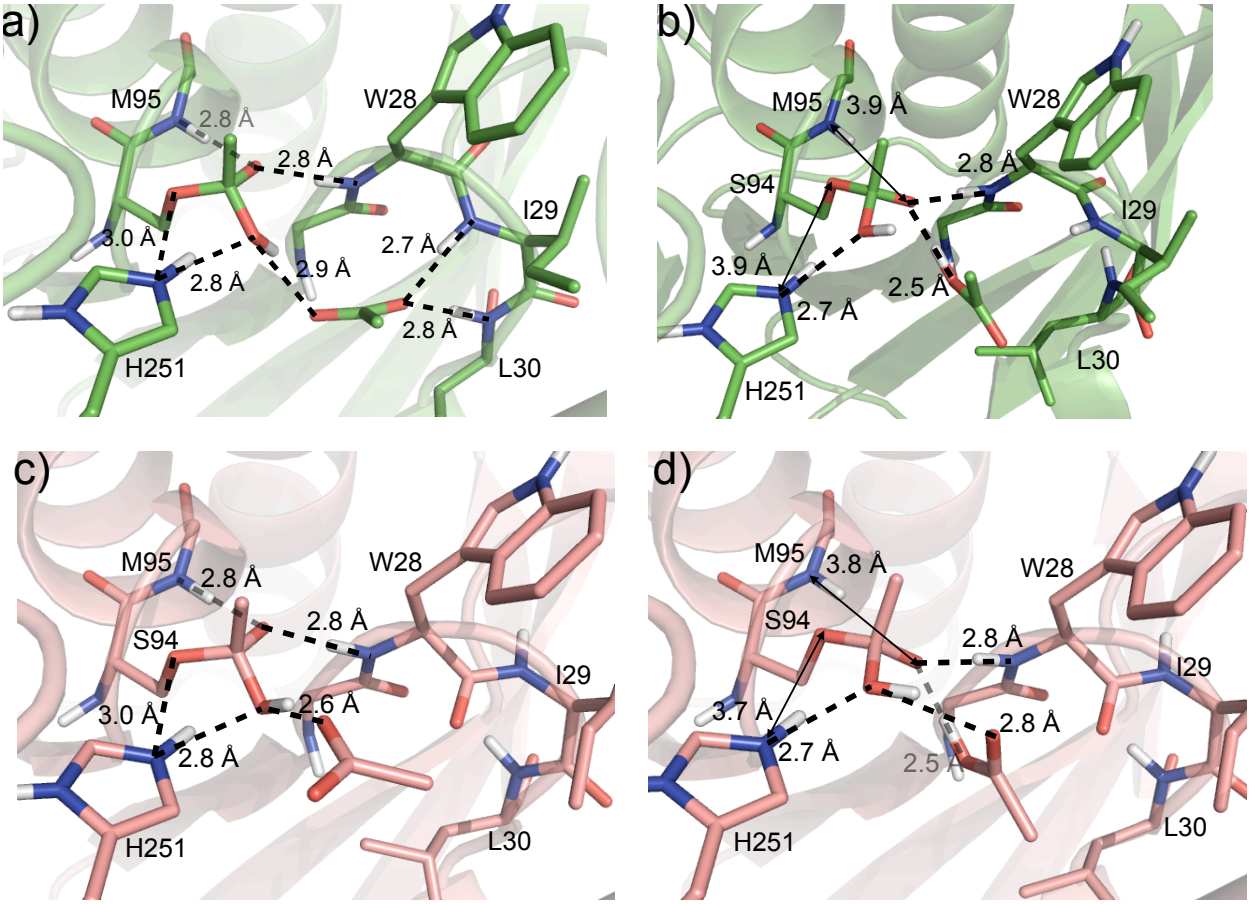

Figure S4. Molecular modeling predicts L29I-T_d1 with type I turn and a bound acetate forms the acetyl enzyme intermediate faster than structures with a type II turn or with bound acetic acid. Starting from the crystal structure L29I/acetate, the acetic acid nearest to the oxyanion hole was

covalently linked to the active site serine to form a tetrahedral intermediate. The top row represents the L29I with a type I using either acetate a) or acetic acid b). The bottom row represents L29I with a type II turn in the oxyanion loop using either acetate c) or acetic acid d). The acetic acid structures b) and d) show a disrupted oxyanion hole because acetic acid hydrogen bonds to the oxyanion oxygen of T_d1. The type II turn structure with bound acetate shows a catalytically productive interaction, but there are no additional interactions that could hold the acetate in place.

The three other T_d1 models lack one or more hydrogen bonds and are not catalytically productive. The type I turn of L29I-T_d1 intermediate with acetic acid, Figure S4b, is missing two catalytically important hydrogen bonds: His-NεH does not donate a hydrogen bond to Ser-Oγ and the main chain amide of M95 does not donate a hydrogen bond to the oxyanion. The unionized form of ACT2 is in a different orientation than the ionized form seen in the type I turn structure. In Figure S4b, ACT2 donates a hydrogen bond to the oxyanion, but the carboxylate oxygen does not accept a hydrogen bond to either main chain amide of I29 or L30.

In the type II turn of L29I-Td1 intermediate with acetate, Figure S4c, the ionized form of ACT2 does not accept a hydrogen bond from the main chain amide of L30; ACT2 cannot accept a hydrogen bond with the main chain amide of L29 since the oxyanion loop is a type II turn. Although Figure S4c shows ACT2 accepting a hydrogen bond from T_d1-OH, there are no hydrogen bond donors present to hold ACT2 in position. Without hydrogen bond donors to position ACT2, it is unlikely that the orientation of the acetic acid molecule could be stable enough for catalysis. The other catalytically productive hydrogen bonds are all present: the oxyanion of the tetrahedral intermediate accepts two hydrogen bonds from the main chain amides (M95 and W28), the His-NεH donates a hydrogen bond to hydroxyl group of the tetrahedral intermediate (T_d1-OH) and to Ser-Oγ.

The type II turn of L29I-Td1 intermediate with acetic acid (Figure S4d) lacks two of the four catalytically important hydrogen bonds: His-NεH does not donate a hydrogen bond to Ser-Oγ and the main chain amide of M95 does not donate a hydrogen bond to the oxyanion. However, ACT2 can donate a hydrogen bond to the oxyanion while the carboxylate group of ACT2 can accept a hydrogen bond from T_d1-OH. This structure neither gains or loses hydrogen bonds.

Supplemental References

[1] P. Bernhardt, K. Hult, R. J. Kazlauskas, *Angew. Chem., Int. Ed. Engl.* **2004**, *44*, 2742–2746.

[2] D. L. Yin, P. Bernhardt, K. L. Morley, Y. Jiang, J. D. Cheeseman, V. Purpero, J. D. Schrag, R. J. Kazlauskas, *Biochemistry* **2010**, *49*, 1931–1942.

[3] D. L. Yin, R. J. Kazlauskas, *Chem. Eur. J.* **2012**, *18*, 8130–8139

[4] D. E. Metzler, Chapter 2: Amino acids, peptides and proteins, in *Biochemistry: the Chemical Reactions of Living Cells*, 2nd ed., Vol. 1, Harcourt/Academic Press, San Diego, CA, p 41.

[5] W. L. Jorgensen, D. S. Maxwell, J. Tirado-Rives, *J. Am. Chem. Soc.* **1996**, *118*, 11225–11236.